First evidence of γ collectivity close to the doubly magic core ^{132}Sn

W. Urban,[1] K. Sieja,[2,3] T. Rząca-Urban,[1] M. Czerwiński,[1] H. Naïdja,[2,3,4,5] F. Nowacki,[2,3] A. G. Smith,[6] and I. Ahmad[7]
[1]*Faculty of Physics, University of Warsaw, Ulica Pasteura 5, PL-02-093 Warsaw, Poland*
[2]*Université de Strasbourg, IPHC, 23 Rue du Loess, F-67037 Strasbourg, France*
[3]*CNRS, UMR7178, F-67037 Strasbourg, France*
[4]*GSI Helmholtzzentrum für Schwerionenforschung GmbH, D-64291 Darmstadt, Germany*
[5]*Université Constantine 1, LPMS, Route Ain-El Bey, 25000 Constantine, Algeria*
[6]*Department of Physics and Astronomy, The University of Manchester, M13 9PL Manchester, United Kingdom*
[7]*Argonne National Laboratory, Argonne, Illinois 60439, USA*
(Received 7 December 2015; published 21 March 2016)

The ^{138}Te and ^{140}Xe nuclei have been reinvestigated using prompt γ-ray data from spontaneous fission of ^{248}Cm, collected with the EUROGAM2 Ge array. γ bands have been identified in both nuclei. The γ band observed in ^{138}Te, a nucleus with only six valence nucleons, indicates the presence of collectivity very close to the doubly magic ^{132}Sn core. Such band is even more pronounced in ^{140}Xe, the $N = 86$ isotone of ^{138}Te. The newly observed bands are interpreted within the shell model, which reproduce well the γ collectivity at $N = 86$.

DOI: 10.1103/PhysRevC.93.034326

I. INTRODUCTION

One of the goals of nuclear structure studies is to search for mechanisms creating the collectivity in atomic nuclei and understanding them in terms of the underlying shell structure. Recently, both the calculations [1] and the experiments [2,3] indicated that quadrupole collectivity can develop when just a few particles are added to the ^{78}Ni core. Four protons or neutrons in the valence space allow for the realization of the pseudo-SU(3) scheme which leads to deformed configurations, showing also the possibility of K mixing, thus, of nonaxial shapes.

One may ask if a similar effect should be present in the vicinity of the doubly magic core ^{132}Sn. Observation of such phenomenon would enable drawing an analogy between the two regions, similar to the known analogy between the ^{132}Sn and ^{208}Pb core regions, and in this way to learn more about the still enigmatic ^{78}Ni core.

Following recent studies of γ collectivity around ^{78}Ni (see works [1–4] and references therein as well as an earlier theoretical study [5]), we have searched for similar effects in nuclei with a few valence nucleons outside the ^{132}Sn core. The present paper reports on the first observation of γ bands close to the ^{132}Sn core, found in the ^{138}Te and ^{140}Xe, $N = 86$ isotones.

In Sec. II we describe the experiment and data analysis and present excitation schemes of ^{138}Te and ^{140}Xe. In Sec. III the newly observed γ bands are interpreted using the shell model. Section IV concludes the work.

II. EXPERIMENT AND DATA ANALYSIS

To search for new excitations in ^{138}Te and ^{140}Xe we used multiple-γ coincidence data collected with the EUROGAM2 Ge-detector array [6], in a measurement of prompt γ radiation, following spontaneous fission of ^{248}Cm. The experiment was described previously in a number of articles and we refer the reader to Ref. [7] for more experimental details. The data have been sorted within the time window of 400 ns into three-dimensional (3D) histograms of high dispersion [8], which allowed further progress as compared to an early analysis done for ^{138}Te [9] and ^{140}Xe [10–12].

A. Level scheme of ^{138}Te

The identification of excited levels in ^{138}Te was made in Ref. [9], using mass correlation based on the analysis of prompt-γ spectra gated on lines from complementary fission fragments of ruthenium nuclei, produced in spontaneous fission of ^{248}Cm. This was later confirmed in Ref. [13] by another mass correlation. In the present work we gated on the known lines of ^{138}Te, reported in Ref. [9] to search for new lines in this nucleus.

Figure 1 shows a γ spectrum, doubly gated on the 443.2- and 461.1-keV lines of ^{138}Te [9] in a triple-γ histogram. In the spectrum there are known lines of ^{138}Te [9] at 535.5, 649.2, 671.8, and 759.9 keV, known lines of the complementary fragments ^{106}Ru and ^{108}Ru as well as candidates for new lines in ^{138}Te, seen at 389.3, 584.9, 869.9, and 1247.7 keV. A spectrum doubly gated on the 389.3- and 759.9-keV lines, displayed in Fig. 2 shows new lines at 139.9 and 479.7 keV and a spectrum in Fig. 3, gated on the 535.5- and 584.9-keV lines shows new lines at 262.8, 271.5, 394.8, and 728.2 keV. The 535.5-keV line appears to be a triplet, as found in other gates. These spectra and further gating allowed in the present work the extension of the level scheme of ^{138}Te as shown in Fig. 4. In Table I we show properties of γ lines in ^{138}Te, populated in spontaneous fission of ^{248}Cm, as seen in this work.

A recent work [14] has reported low-spin excited levels in ^{138}Te, populated in β decay of ^{138}Sb. In this work the order of the 443.2- and 461.1-keV transitions was reversed, as compared to the order reported in Ref. [9], introducing the 2^+ level at 461.1 keV instead of 443.2 keV. We confirm the proposition of Ref. [14]. In the ^{108}Ru nucleus, populated in fission of ^{248}Cm as the most abundant fission fragment complementary to ^{138}Te (4n channel), there is a 443-keV transition [15]. This transition not known at the time of ^{138}Te

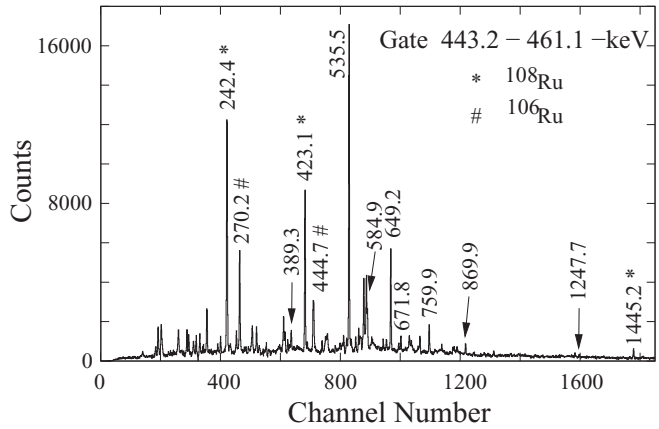

FIG. 1. γ spectrum doubly gated on known 443.2- and 461.1-keV lines of ^{138}Te in the data from the ^{248}Cm spontaneous fission. Arrows indicate new lines in ^{138}Te.

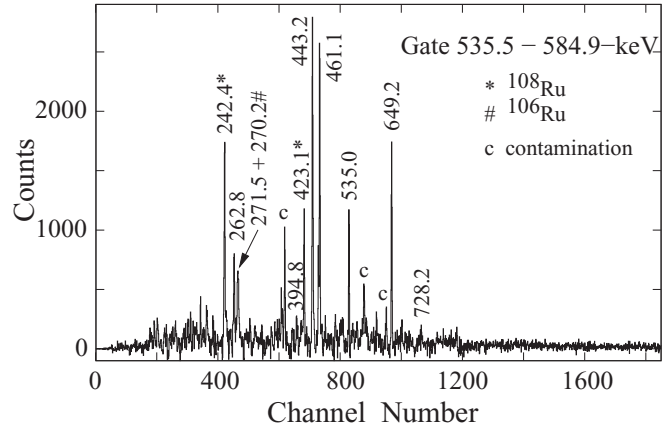

FIG. 3. γ spectrum doubly gated on the new 584.9-keV line and the known 535.5-keV line of ^{138}Te, in the data from the ^{248}Cm spontaneous fission.

analysis reported in Ref. [9], artificially raises the intensity of the 443-keV line seen in ^{138}Te. The corrected intensity, shown in Table I indicates that the 443.2-keV transition is weaker than the 461.1-keV transition.

Crucial for the interpretation of the observed levels are spin and parity assignments. In the present work we have determined angular correlations for some of the $\gamma\gamma$ cascades, using techniques described in Ref. [7]. It is known that an intermediate, stretched quadrupole transition in a cascade does not change angular correlations. Therefore, we used summed γ spectra which provided higher count rates. We have also checked that all transitions observed in ^{138}Te in this work are of prompt character, with the upper limit of lifetimes of excited levels seen here as 10 ns, which in some cases excludes $M2$ multipolarity, as discussed below.

The results, shown in Table II, combined with the predominant population of yrast levels in fission fragment nuclei [16] and the observed decay branchings, allowed spin and parity assignments to levels in ^{138}Te, as shown in Fig. 4. Details of these assignments are discussed below.

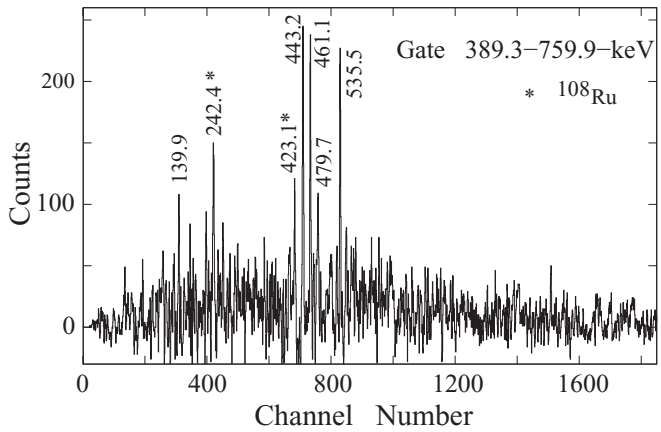

FIG. 2. γ spectrum doubly gated on the known 759.9-keV line and the new 389.3-keV line of ^{138}Te, in the data from the ^{248}Cm spontaneous fission.

The assignments of spins $I = 2$, 4, 6, 8, and 10 to the 461.1-, 904.3-, 1439.8-, 2089.0- and 2760.8-keV levels of the ground-state band are consistent with the angular correlations shown in Table II and the yrast-population argument. The prompt character of the decays in the cascade is consistent with their stretched $E2$ character, thus positive parity of the discussed levels.

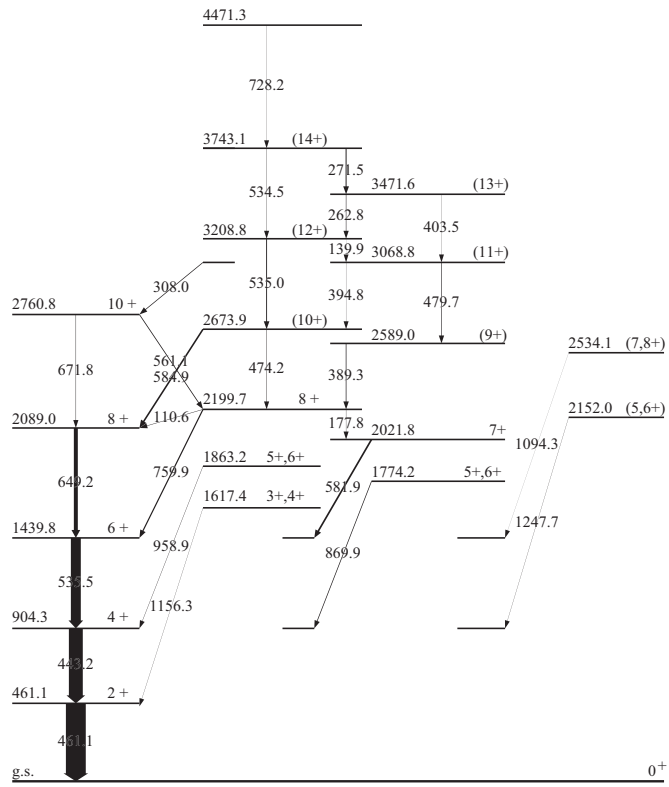

FIG. 4. Level scheme of ^{138}Te deduced in the present work.

TABLE I. Properties of γ transitions in ^{138}Te as observed in the present work following spontaneous fission of ^{248}Cm. The I_γ values are in arbitrary, relatives units.

$E_\gamma(\Delta E_\gamma)$ (keV)	$I_\gamma(\Delta I_\gamma)$ (rel.)	$E^{\rm exc}_{\rm init.}$ (keV)	$E_\gamma(\Delta E_\gamma)$ (keV)	$I_\gamma(\Delta I_\gamma)$ (rel.)	$E^{\rm exc}_{\rm init.}$ (keV)
110.6(2)	2.4(3)	2199.7(3)	535.0(4)	3(1)	3208.8(5)
139.9(3)	0.6(2)	3208.8(5)	535.5(1)	48(5)	1439.8(3)
177.8(2)	1.8(4)	2199.7(3)	561.1(1)	3.8(3)	2760.8(4)
262.8(2)	2.6(4)	3471.6(6)	581.9(2)	8.5(7)	2021.8(3)
271.5(2)	1.8(4)	3743.1(7)	584.9(1)	8.8(7)	2673.9(3)
308.0(2)	3.4(4)	3068.8(4)	649.2(1)	19.0(9)	2089.0(3)
389.3(1)	3.5(4)	2589.0(4)	671.8(1)	2.1(4)	2760.8(4)
394.8(3)	0.7(3)	3068.8(4)	728.2(3)	1.3(4)	4471.3(8)
403.5(4)	1.0(3)	3471.6(6)	759.9(1)	5.8(3)	2199.7(3)
443.2(1)	85(7)	904.3(2)	869.9(2)	3.2(4)	1774.2(3)
461.1(1)	100(3)	461.1(1)	958.9(2)	1.6(4)	1863.2(3)
474.2(2)	1.8(3)	2673.9(3)	1094.3(4)	0.05(2)	2534.1(5)
479.7(2)	3.0(3)	3068.8(4)	1156.3(3)	0.07(3)	1617.4(4)
534.5(4)	0.5(3)	3743.1(7)	1247.7(3)	0.08(2)	2152.0(4)

Angular correlations for the 759.9-keV line are consistent with its stretched quadrupole character, thus spin and parity 8^+ of the 2199.7-keV level. Spin and parity 8^+ is further confirmed by the 561.1-keV decay from the 2760.8-keV level, having spin and parity 10^+.

For the 581.9-keV line angular correlations provide two solutions, with spin either 6 or 7 for the 2021.8-keV level. Spin 7 is favored by the low-energy decay from the 2199.7-keV level to the 2021.8-keV level. The corresponding mixing coefficient, $\delta = 0.11(3)$, for the 581.9-keV transition indicates its $M1+E2$ multipolarity and, therefore, positive parity of the 2021.8-keV level.

The angular correlation for the 389.3-keV line is consistent with spin $I = 9$ assignment to the 2589.0-keV level. The nonzero mixing coefficient of the 389.3-keV transition suggests its $M1+E2$ multipolarity, thus positive parity for the 2589.0-keV level.

The angular correlation for the 308.0-keV line is consistent with spin $I = 11$ assignment to the 3068.8-keV level. The nonzero mixing coefficient of the 308.0-keV transition suggests its $M1+E2$ multipolarity, thus positive parity for the 3068.8-keV level.

The yrast population argument and the prompt character of the 139.9-, 403.5-, 262.8-, 271.5-, and 534.5-keV decays suggest positive parity and spins 12, 13, and 14 for the 3208.8-, 3471.6-, and 3743.1-keV levels, respectively.

The angular correlation for the 869.9-keV line is consistent with the 5^+ or 6^+ spin and parity assignment to the 1774.2-keV level (large, positive anisotropy excludes $I^\pi = 5^-$ assignment).

Considering the observed decay branches, the yrast population argument, and the prompt character of the observed decays, we tentatively propose spin 3 or 4+ for the 1617.4-keV level, spin 5 or 6+ for the 1863.2-keV level, spin 5 or 6^+ for the 2152.0-keV level, and spin 7 or 8+ for the 2534.1-keV level.

The observation of the 1617.4-keV level (1615.3 keV in Ref. [14]) and the nonobservation of other, nonyrast levels reported in Ref. [14] favors spin 4^+ for the 1617.4-keV level and spins 2^+ or 3^+ for other nonyrast levels reported in Ref. [14].

It should be noted that the arrangement of levels into bands, as shown in Fig. 4, is somewhat arbitrary, especially for levels with two possible spin values or the two 10^+ levels. This is discussed further in Sec. III.

B. Level scheme of ^{140}Xe

Over 20 yrast excitations in the ^{140}Xe fission fragment, well populated in spontaneous fission of ^{248}Cm, have been reported by Bentaleb *et al.* [10], using the EUROGAM1 array. These results have been confirmed and extended in a study of ^{252}Cf fission [11], where an octupole band in ^{140}Xe was suggested. The subsequent measurement of ^{248}Cm, made with the EUROGAM2, has confirmed that the side bands in ^{140}Xe, reported in Refs. [10,11], is an octupole band [12]. We now use the same data set with improved analysis techniques to

TABLE II. Experimental angular correlation coefficients A_k/A_0, and the corresponding mixing coefficients δ for γ lines in ^{138}Te, as obtained in the present work. "Sum" indicates correlation of the γ line determined from a spectrum being a sum of γ spectra gated on lines in the cascade below the line of interest.

Cascade E^a_γ - E_γ	A_2/A_0	A_4/A_0	Spin hypothesis	$\delta(\gamma^{\rm a})$
308.0 - Sum	0.075(43)	0.0159(70)	11 → 10 - Sum	0.25(9)
389.3 - Sum	0.010(19)	0.016(31)	9 → 8 - Sum	0.10(3)
461.1 - 443.2	0.101(8)	0.032(15)	4 → 2 - 2 → 0	0
535.5 - 443.2	0.107(10)	−0.016(18)	6 → 4 - 2 → 0	0
581.9 - Sum	−0.002(19)	0.017(28)	7 → 6 - Sum	0.11(3)
			6 → 6 - Sum	0.67(8)
649.2 - 443.2	0.128(34)	0.034(52)	8 → 6 - 2 → 0	0
649.2 - Sum	0.099(19)	0.015(30)	8 → 6 - Sum	0
671.8 - Sum	0.118(71)	−0.001(118)	10 → 8 - Sum	0
759.9 - Sum	0.102(31)	0.031(49)	8 → 6 - Sum	0
869.9 - Sum	0.215(35)	−0.067(65)	5 → 4 - Sum	−0.1(1)

[a]Indicates γ transition for which the mixing was determined.

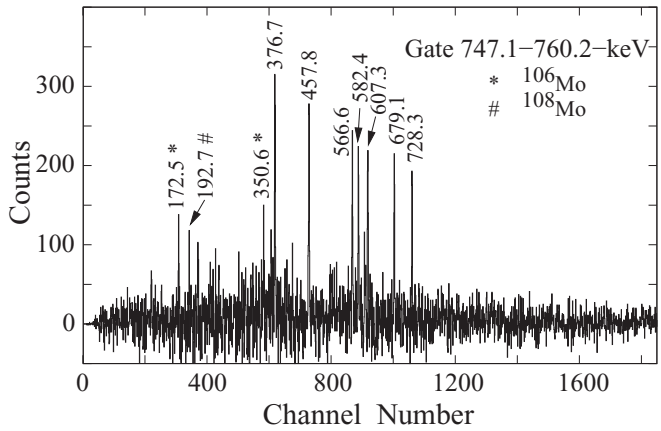

FIG. 5. γ spectrum doubly gated on the known 747.1- and the new 760.2-keV lines of ^{140}Xe in the data from the ^{248}Cm spontaneous fission.

explain the nature of other side bands in ^{140}Xe, reported in Refs. [10,11].

Figure 5 shows γ spectrum doubly gated on the two highest 747.1- and 760.2-keV lines in the ground-state band of ^{140}Xe, reported in Ref. [12], illustrating the quality of the data.

The new level scheme of ^{140}Xe, as obtained in this work is shown in Fig. 6 and the properties of γ transitions of ^{140}Xe are listed in Table III, where we give precise energy values, which are rounded to one digit after the decimal point in Fig. 6, to simplify the complex drawing.

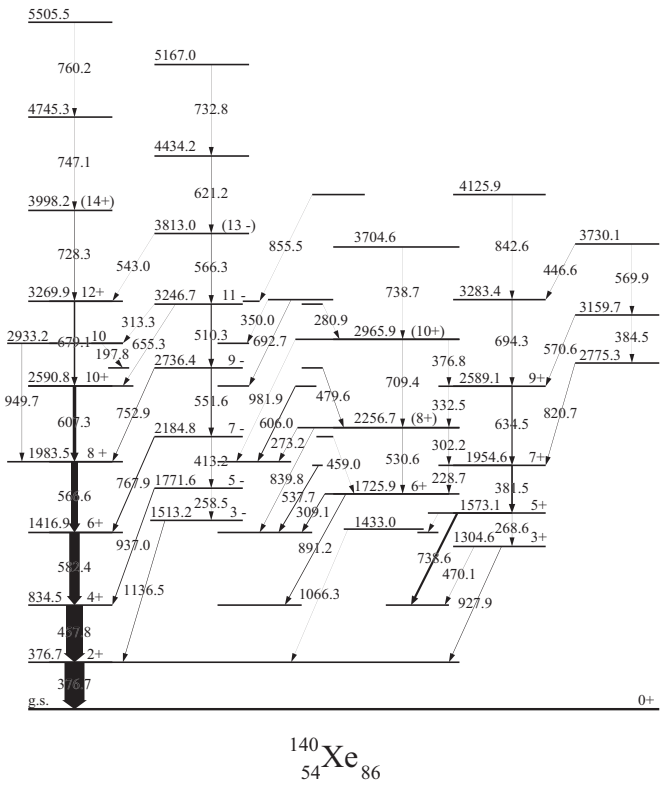

FIG. 6. Partial level scheme of ^{140}Xe deduced in the present work.

TABLE III. Properties of γ transitions in ^{140}Xe as observed in the present work in the spontaneous fission of ^{248}Cm. The I_γ values are in arbitrary, relative units.

$E_\gamma(\Delta E_\gamma)$ (keV)	$I_\gamma(\Delta I_\gamma)$ (rel.)	$E^{ex}_{init.}$ (keV)	$E_\gamma(\Delta E_\gamma)$ (keV)	$I_\gamma(\Delta I_\gamma)$ (rel.)	$E^{ex}_{init.}$ (keV)
156.3(1)	0.32(5)	1573.1	570.55(10)	1.5(2)	3159.7
197.8(2)	0.3(1)	2933.2	582.44(5)	54(2)	1416.9
228.70(7)	0.9(1)	1954.6	606.0(3)	3(1)	2589.1
258.5(2)	0.2(1)	1771.6	607.25(5)	18(1)	2590.8
268.60(6)	0.9(1)	1573.1	621.2(1)	1.7(2)	4434.2
273.24(6)	1.2(1)	2256.7	634.50(5)	5.9(4)	2589.1
280.92(21)	0.4(2)	3246.7	655.3(3)	0.7(1)	3246.7
302.22(9)	0.5(1)	2256.7	679.11(5)	6.7(3)	3269.9
309.10(5)	4.0(2)	1725.9	692.6(1)	1.3(2)	3283.4
313.3(2)	0.3(1)	3246.7	694.26(6)	1.6(2)	3283.4
332.5(2)	0.2(1)	2589.1	709.40(15)	0.7(2)	2965.9
350.0(4)	0.2(1)	3283.4	728.25(6)	1.6(2)	3998.2
376.66(5)	100(3)	376.7	732.80(8)	0.9(1)	5167.0
376.8(2)	0.3(1)	2965.9	738.64(5)	10.6(5)	1573.1
381.48(5)	8.2(4)	1954.6	738.7(3)	0.2(1)	3704.6
384.45(15)	0.3(1)	3159.7	747.13(9)	0.32(5)	4745.3
413.20(7)	1.5(1)	2184.8	752.85(5)	2.6(2)	2736.4
446.6(1)	0.5(1)	3730.1	760.22(24)	0.17(4)	5505.5
457.78(5)	87(3)	834.5	767.92(5)	5.0(2)	2184.8
459.0(2)	0.3(1)	2184.8	820.68(7)	1.6(2)	2775.3
470.10(9)	0.9(2)	1304.6	839.79(7)	1.5(2)	2256.7
479.55(8)	2.0(2)	2736.4	842.6(1)	0.4(1)	4125.9
510.30(6)	5.5(5)	3246.7	855.5(3)	0.2(1)	4125.9
530.55(12)	1.1(2)	2256.7	891.20(7)	3.2(2)	1725.9
537.70(5)	4.1(2)	1954.6	927.90(9)	2.6(2)	1304.6
543.0(3)	0.2(1)	3813.0	937.03(5)	3.7(2)	1771.6
551.64(5)	5.1(3)	2736.4	949.70(6)	0.9(1)	2933.2
566.25(7)	2.4(3)	3813.0	981.9(2)	0.31(5)	2965.9
566.64(5)	35(1)	1983.5	1066.3(3)	0.2(1)	1433.0
569.9(2)	0.3(2)	3730.1	1136.52(15)	1.2(2)	1513.2

In Table IV we show the results of angular-correlation measurement made with the EUROGAM2 array for γ lines of ^{140}Xe. Because of the high population of ^{140}Xe in fission of ^{248}Cm, the accuracy of these correlations is high, as illustrated in the top five rows of the table. In the first three rows we show angular correlations for the 376.7-, 457.8-, and 582.4-keV lines, corresponding to the strongest quadrupole transitions in ^{140}Xe. The correlations have been obtained from a γ spectrum, denoted Sum3, which is a sum of three spectra, gated on these three lines. The theoretical A_k/A_0 coefficients in a cascade of two stretched, quadrupole transitions is $A_2/A_0 = 0.102$ and $A_4/A_0 = 0.009$, in excellent agreement with the experimental coefficients for the 376.7-, 457.8-, and 582.4-keV transitions. In addition, we show in the next two rows angular correlations, found in the same Sum3 spectrum, for lines of the complementary ^{108}Mo fission fragment. As expected, the anisotropy is zero.

Below we briefly describe how the excitation scheme of ^{140}Xe was constructed and discuss spin and parity assignments in this nucleus.

Angular correlations confirm the stretched quadrupole multipolarity of transitions in the ground-state band up to

TABLE IV. Experimental angular correlation coefficients and the corresponding mixing coefficients δ for γ transitions in ^{140}Xe, as obtained in the present work. "Sum" indicates correlation of the γ line determined from a spectrum being a sum of γ spectra gated on γ lines in the cascade below. "Sum3" indicates correlation of the γ line determined from a spectrum being a sum of γ spectra gated on the 376.6-, 457.6- and 582.4-keV γ lines.

Cascade E_γ^a - E_γ	A_2/A_0	A_4/A_0	Spin hypothesis	$\delta(\gamma^a)$
376.7 - Sum3	0.104(2)	0.012(3)	4 → 2 - Sum3	0
457.8 - Sum3	0.104(5)	0.007(7)	4 → 2 - Sum3	0
582.4 - Sum3	0.103(5)	0.022(8)	4 → 2 - Sum3	0
192.3 - Sum3	0.004(6)	0.007(9)	4 → 2 - Sum3	
369.0 - Sum3	0.003(5)	−0.002(7)	4 → 2 - Sum3	
309.1 - Sum	0.204(5)	−0.012(8)	6 → 6 - Sum	0.48(4)
			5 → 6 - Sum	−0.23(2)
381.5 - 738.6	0.126(5)	−0.009(8)	7 → 5 - 5 → 4	0
738.6 - 381.5	0.126(5)	−0.009(8)	7 → 5 - 5 → 4	0.51(3)
457.8 - 376.7	0.104(5)	0.007(7)	4 → 2 - 2 → 0	0
470.1 - Sum	−0.045(13)	0.003(22)	2 → 4 - Sum	No solut.
			3 → 4 - Sum	−0.11(2)
			4 → 4 - Sum	0.67(5)
566.6 - Sum	0.100(4)	0.017(7)	8 → 6 - Sum	0
582.4 - 457.8	0.104(6)	0.015(9)	6 → 4 - 4 → 2	0
607.3 - Sum	0.060(4)	0.043(8)	12 → 10 - Sum	0
634.5 - 381.5	0.099(13)	0.037(22)	9 → 7 - 7 → 5	0
679.1 - Sum	0.091(10)	−0.012(16)	12 → 10 - Sum	0
728.3 - Sum	0.064(14)	−0.119(24)	14 → 12 - Sum	0
			13 → 12 - Sum	3.0(3)
738.6 - Sum	0.189(5)	−0.017(8)	4 → 4 - Sum	−0.03(2)
			5 → 4 - Sum	0.50(2)
			6 → 4 - Sum	No solut.
738.6 - 381.5	0.125(8)	-0.010(11)	5 → 4 - 7 → 5	0.51(2)
752.9 - Sum	−0.066(11)	0.016(17)	9 → 8 - Sum	0.007(14)
767.9 - Sum	−0.065(9)	−0.008(16)	7 → 6 - Sum	0.01(2)
891.1 - Sum	0.100(35)	0.065(58)	6 → 4 - Sum	0
			5 → 4 - Sum	0.28(7)
927.9 - 376.7	0.254(23)	0.058(43)	2 → 4 - 2 → 0	−0.01(3)
			3 → 4 - 2 → 0	0.61(15)
			4 → 4 - 2 → 0	No solut.
937.0 - Sum	−0.062(14)	−0.005(23)	5 → 4 - Sum	0.02(2)

[a]Indicates γ transition for which the mixing was determined.

spin $I = 12$. Angular correlation of the 607.3-keV transition is affected by the 606.0-keV transition. For the 728.3-keV transition we cannot exclude its $\Delta I = 1$ character, which is, however, less likely, considering very large mixing ratio corresponding to this solution.

The level at 2933.2 keV, proposed previously in Ref. [11], most likely has spin $I = 10$, as concluded from its decay and feeding branches but the parity could not be deduced in the present work.

We confirm the octupole band, reported in Ref. [12], adding the 732.8-keV transition at the top of the band and the 280.9-, 313.3-, 459.0-, and 479.6-keV decays off the band. The present angular correlations for the 752.9-, 767.9-, and 937.0-keV decays of the 2736.4-, 2184.8-, and 1771.6-keV levels, respectively, confirm spin and parity assignments of 9^-, 7^-, and 5^- to these levels, respectively, with higher accuracy than Ref. [12].

Two side bands in ^{140}Xe, reported in Ref. [10], based on the 1304.3- and 1725.3-keV levels, respectively, have been rearranged because of new transitions of 280.9, 332.5, 350.0, 376.8, 446.6, 459.0, 470.1, 479.6, 694.3, 709.4, 738.7, 842.6, 855.5, and 981.9 keV, observed in the present work. We propose that the two side bands form one band of levels interconnected by low-energy transitions.

The angular correlation for the 738.6-keV transition indicates spin 4 or 5 for the 1573.1-keV level. For the spin 6 hypothesis there is no solution. The large positive anisotropy and large mixing coefficient excludes an $I^\pi = 5^-$ assignment to this level. The prompt-γ, 156.3-keV decay from the 1573.1-keV level to the 6^+, 1416.9-keV level makes the spin $I = 4$ assignment unlikely. With spin $I = 4$ a quadrupole decay of 1196.4 keV to the 376.7-keV level should be much stronger than the quadrupole decay of 156.3 keV to the 1416.9-keV level, which is not the case (the 1196.4-keV transition is not

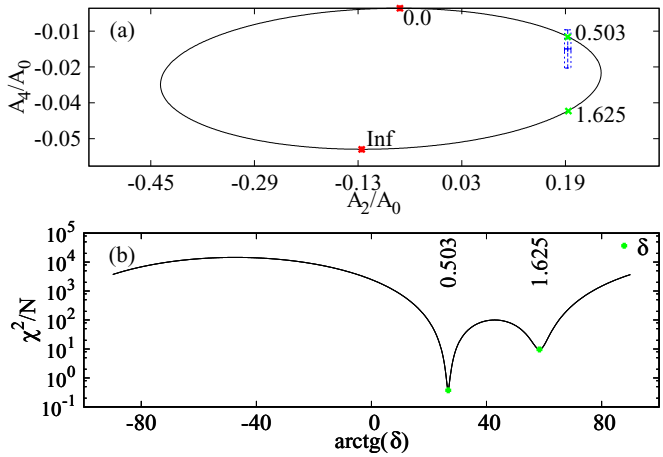

FIG. 7. Angular correlation analysis for the 738.6-Sum cascade in ^{140}Xe with spin $I = 5$ hypothesis for the 1573.1-keV level. Blue box in (a) represents the experimental data point with error bars, while the green dots indicate solutions for A_k/A_0 and δ coefficients. (b) Shows the associated Chi-square plot.

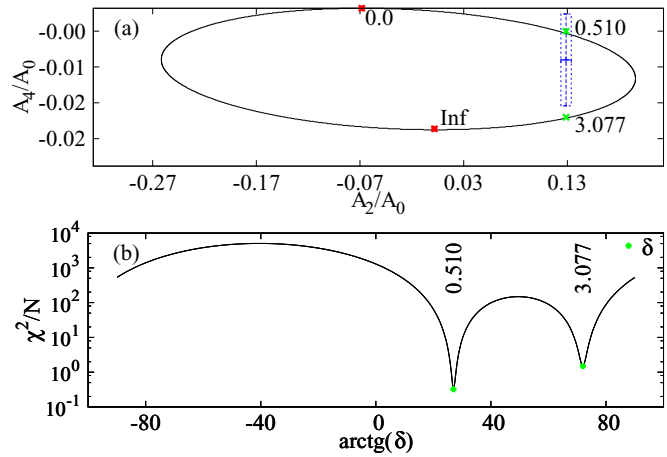

FIG. 8. Angular correlation analysis for the 381.5- to 738.6-keV cascade in ^{140}Xe with the spin $I = 7$ hypothesis for the 1954.6-keV level.

seen in this work). This leaves the unique spin and parity assignment of 5^+ to the 1573.1-keV level. Figure 7 illustrates the angular-correlation analysis for the 738.6-Sum cascade with the spin $I = 5$ hypothesis for the 1573.1-keV level.

Analogous analysis performed for the 927.9-keV transition gives a spin and parity assignment of 3^+ to the 1304.6-keV level. Here, the angular correlation for the 927.9-keV transition allows spin 2 or 3, while the correlation for the 470.1-keV transition allows spin 3 or 4, leaving spin 3 as the only common solution for the 1304.6-keV level. Clearly, the nonzero mixing coefficient indicates an $M1+E2$ character of both transitions, thus positive parity for this level.

The angular correlation for the 891.2-keV transition allows spin 5 or 6 for the 1725.9-keV level. For the $I = 5$ solution the large mixing coefficient indicates positive parity for this level. However, in this case the 459.0-keV decay from the 7^-, 2184.8-keV level should have an $M2$ multipolarity, consistent only with a microsecond partial half-life for this decay. Because this is not observed we reject the $I = 5$ spin assignment. Thus spin of the 1725.9-keV level is $I = 6$. Positive parity is indicated by the angular correlation of the 309.1-keV transition and its $M1+E2$ multipolarity.

The angular correlation for the 381.5- to 738.6-keV cascade indicates uniquely a stretched quadrupole character of the 381.5-keV transition, thus, spin and parity 7^+ for the 1954.6-keV level, when the mixing coefficient $\delta = 0.50$ obtained above, is adopted for the 738.6-keV transition. To check the consistency of these angular correlations we have performed an analysis for the 738.6- to 381.5-keV cascade assuming a stretched quadrupole character for the 381.5-keV transition and searching for the mixing coefficient δ of the 738.6-keV transition. The analysis shown in Fig. 8 agrees well with the result in Fig. 7, giving $\delta = 0.51$.

The angular correlation for the 634.5- to 381.5-keV cascade, is consistent with both transitions being stretched quadrupoles, supporting spin and parity 9^+ for the 2589.1-keV level.

For the 2256.7- and 2965.9-keV levels, tentative 8^+ and 10^+ spin and parity assignments are proposed, respectively, considering the observed feeding and decay branches, the prompt character of the observed transitions, and using the yrast-population argument.

The new 1433.0-keV level may have spin 3 or 4, considering its decay.

III. DISCUSSION

A. Excitations in $N = 86$ isotones

Until now the collective structure closest to the ^{132}Sn core was the octupole band in ^{140}Xe [12]. Such bands develop quickly when particles are added to the low-spin member of the $\Delta I = 3$, $\Delta\pi = -1$ pair of orbitals ($\nu g_{7/2}$ or $\pi d_{5/2}$ in the ^{132}Sn region). Figure 9(a) shows the systematics of known negative-parity levels in even-Z, $N = 86$ isotones, associated with octupole bands in the even-Z, $N = 86$ isotones [12,17,18].

In ^{140}Xe the octupole band is well developed while the existing data do not provide any evidence for an octupole band in ^{138}Te. However, the present work indicates possible quadrupole collectivity present in ^{138}Te. The trend shown in Fig. 9(b) by filled squares, representing ground-state-band levels, varies smoothly from ^{150}Gd down to ^{138}Te. Excitation energies of these levels are characteristic of collective vibrations, with the maximum collectivity around ^{142}Ba, when judged by excitation energies. It is only the ^{136}Sn nucleus, where the pattern of 2_1^+, 4_1^+, and 6_1^+ levels is different, being characteristic of single-particle excitations, corresponding to breaking of the $f_{7/2}$ neutron pair.

Furthermore, open squares in Fig. 9(b) indicate another family of positive-parity levels, comprising both even- and odd-spin values. Such a sequence with low-lying 3^+, 5^+, and 7^+ levels is characteristic of a γ band, as observed recently around the ^{78}Ni core [1,3,4]. In ^{140}Xe, where we have identified low-lying 3^+, 5^+, and 7^+ levels (see Fig. 6), there is a well-developed candidate for a γ band (the 4^+ member of this band still to be confirmed). The excitation scheme of

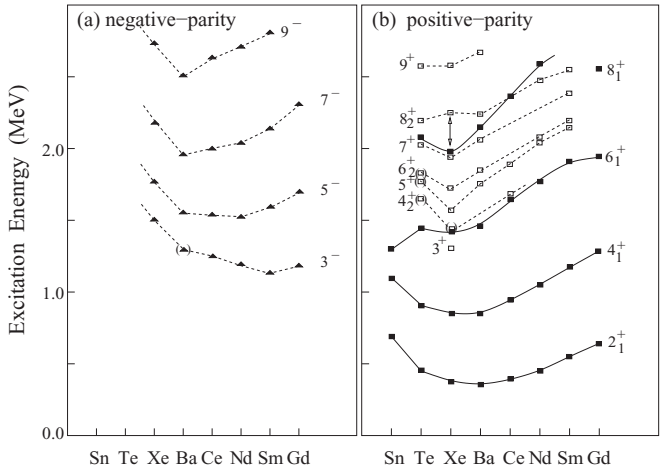

FIG. 9. Systematics of (a) negative-parity and (b) positive-parity levels in even-Z, $N = 86$ isotones. Parentheses indicate tentative spin-parity assignments of $I^\pi = 3^-$ to the 1292.2-keV level in ^{142}Ba, $I^\pi = 4^+$ to the 1433.0-keV level in ^{140}Xe, and $I^\pi = 4^+$, 5^+, and 6^+ to the 1648.0-, 1774.2- and 1863.2-keV levels in ^{138}Te, respectively. The data are taken from this work and Refs. [12,17,18]. Lines are drawn to guide the eye.

^{138}Te, where we have uniquely assigned spin and parity 7^+ to the 2021.8-keV level (see Fig. 4), reveals an analogous band, which we propose as a candidate for a γ band. This and the collective character of the ground-state band discussed above, indicates the presence of quadrupole collectivity in ^{138}Te, only two protons and four neutrons away from the ^{132}Sn core.

A word of caution is in order, concerning the candidate for a γ band in ^{138}Te. As seen in Fig. 4, the (9^+) level at 2589.0 keV does not decay to the 7^+ level at 2021.8 keV, which suggests that the two levels may belong to different structures. In Fig. 9(b) there is an indication of a possible mixing around spin 8^+ (the repulsion between the 8^+ levels). It is possible that the low-spin part of the band belongs to a γ-unstable structure, while around spin 8 this structure mixes with a two-quasiparticle configuration [for example, $\nu(f_{7/2},h_{9/2})_{8^+}$].

B. Shell-model calculations for ^{138}Te and ^{140}Xe

To verify the proposed interpretation of the positive-parity structure observed in ^{138}Te and ^{140}Xe we have performed large-scale, shell-model calculations in a valence space comprising proton $(1g_{9/2},1g_{7/2},2d_{5/2},2d_{3/2},3s_{1/2})$ and neutron $(1h_{11/2},1h_{9/2},2f_{7/2},2f_{5/2},3p_{3/2},3p_{1/2},1i_{13/2})$ orbitals, with the closed $\pi 1g_{9/2}$ and $\nu 1h_{11/2}$ shells (no excitations of the ^{132}Sn core). Effective interaction is based on a realistic N3LO potential, smoothed via $V_{\mathrm{low}k}$ procedure and adapted to the model space by many-body perturbation techniques. Empirical corrections to the realistic potential were applied to reproduce the low-lying levels of $N = 83,84$ isotones. The diagonalization of the shell-model matrices was preformed using the codes ANTOINE and NATHAN [19,20]. In the calculations of $E2$ transition rates, the polarization charge $0.5e$ was used (partial results are discussed in Ref. [21] where further details of the calculations can be found).

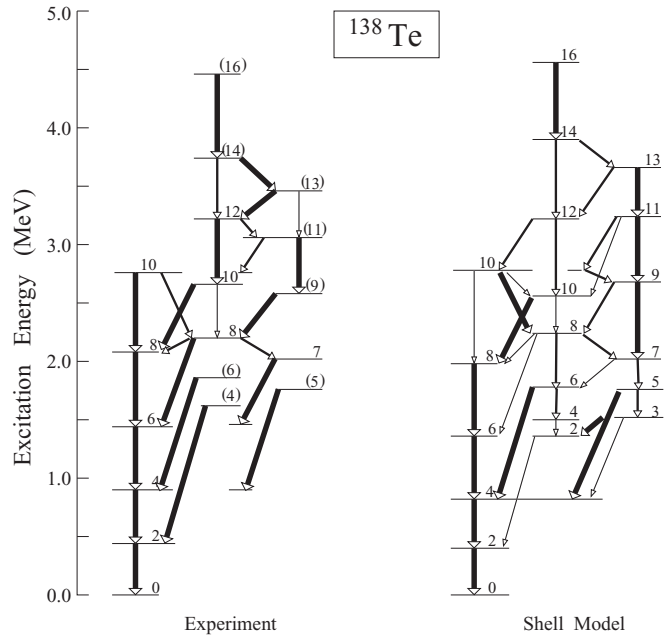

FIG. 10. Experimental positive-parity excitations in ^{138}Te compared to the shell-model calculations performed in the present work. Experimental and calculated data are normalized at the ground state.

The calculated excitation energies for both ^{138}Te and ^{140}Xe nuclei are compared to the respective experimental levels in Figs. 10 and 11. In these figures we also show γ decay branches of excited levels in ^{138}Te and ^{140}Xe, schematically classified as weak, medium, and strong (thin, medium-thick, and thick arrows representing branches of 0%–10%, 10%–30%, and over 30% intensity, respectively). Precise values of calculated electromagnetic moments in both nuclei are shown in Table V.

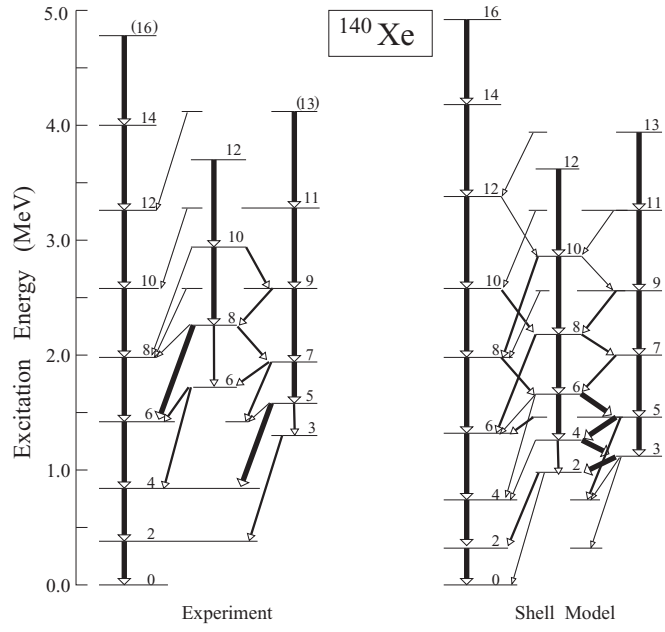

FIG. 11. Experimental positive-parity excitations in ^{140}Xe compared to the shell-model calculations performed in the present work. Experimental and calculated data are normalized at the ground state.

TABLE V. Excitation energies, $B(E2)$ transition rates (in e^2 fm^4), quadrupole moments Q (in e fm^2), and deformation β in ^{138}Te and ^{140}Xe, as obtained from the shell model in this work. $Q_0^{a)}$ moments are obtained from $Q_{\rm spec}$ values and $Q_0^{b)}$ moments are estimated from calculated $B(E2)$ values within the collective model.

Nucleus	J^π	E^* (MeV)	$B(E2)$ J → J-1	$B(E2)$ J → J-2	$Q_{\rm spec}$	$Q_0^{a)}$	$Q_0^{b)}$	β
^{138}Te	2^+	0.41		507	−45	157	160	0.10
	4^+	0.81		731	−61	168	160	0.11
	6^+	1.35		746	−66	166	154	0.11
	8^+	1.99		686	−73	174	145	0.10
	10^+	2.58		561	−79	182	129	0.10
	2_2^+	1.36			38			
	3^+	1.52	770		−3.4			
	4_2^+	1.49	24	43	37			
	5^+	1.75	278	243	4.7			
	6_2^+	1.69	246	71	−12			
	7^+	2.05	4	222	−61			
^{140}Xe	2^+	0.3		1023	−61	214	227	0.14
	4^+	0.72		1468	−79	216	227	0.14
	6^+	1.33		1592	−77	192	225	0.13
	8^+	1.99		1481	−73	173	213	0.12
	10^+	2.68		1341	−82	187	200	0.12
	2_2^+	0.95			62			
	3^+	1.11	1898		−2.2			
	4_2^+	1.25	1331	602	−40			
	5^+	1.44	979	963	−58			
	6_2^+	1.65	759	1012	−83			
	7^+	1.89	468	1101	−85			

As in the case of nuclei above the ^{78}Ni core [1,2,4], the deformation properties of nuclei above the ^{132}Sn core have been also estimated from the pseudo-SU(3) model and are discussed in the text.

In ^{138}Te the assignment of the first and second 10^+ levels to the yrare and yrast bands, respectively, is to some extent, arbitrary. In Fig. 10 there is a link in the experimental scheme between the 12^+ and the 10^+ levels of the yrare band, which we want to maintain. With the second 10^+ level in the yrare band this link would be absent, creating a discontinuity in the yrare band between the 2760.8-keV (10^+) and the 3208.8-keV (12+) levels. On the other hand, the second 10^+ level in the calculated scheme of ^{138}Te decays to the 9^+ level, suggesting the assignment of the second 10^+ to the yrare band. This ambiguity happens in a region of a crossing of the two bands, where the two 10^+ levels are most likely mixed, as indicated by their decays to both 8^+ levels.

Otherwise, there is an overall agreement between theory and experiment for near-yrast structures of ^{138}Te and ^{140}Xe nuclei. Both excitation energies and the majority of decay branches seen in the experiment are well reproduced by the shell model. One should also note that the calculated $B(E2; 2^+ \rightarrow 0^+)$ and $B(E2; 4^+ \rightarrow 2^+)$ values in ^{140}Xe of 24 W.u. and 34 W.u., respectively, match well the experimental ones of 24.9(8) W.u. and 40(9) W.u. reported in Ref. [22].

As can be seen in Table V, the yrast cascade in ^{138}Te is characteristic of a collective band, with somewhat constant intrinsic quadrupole moments Q_0 obtained from the spectroscopic moments and $B(E2)$ transition rates (see Eqs. (9) and (10) of Ref. [1]), up to spin 6^+. We ascribe to this band a modest deformation parameter $\beta = 0.1$. Alternatively, the intrinsic deformation can be estimated by applying the formalism from the multiple-Coulomb-excitations analysis of the $E2$ matrix elements calculated presently with the shell model (see Sec. II.A of Ref. [1] and Ref. [23] for details). Using Eqs. (1)–(3) from Ref. [1] one obtains the intrinsic quadrupole moment of 167 e fm^2 for the ground state of ^{138}Te, close to the estimate from the collective model, as shown in Table V in columns marked $Q_0^{a)}$ and $Q_0^{b)}$. However, both $Q_0^{a)}$ and $Q_0^{b)}$ are lower than the pseudo-SU(3) limit of $Q_0 = 184$ e fm^2, predicted with two protons in the pseudo-gds shell and 4 neutrons in the pseudo-pf shell. This comparison shows that ^{138}Te has not yet reached the rotational limit.

In ^{140}Xe, two more protons added to the $g_{7/2}$ and $d_{5/2}$ shells enhance the collectivity, as compared to ^{138}Te, which can be seen in Table V. The equality of intrinsic quadrupole moments Q_0, calculated from $Q_{\rm spec}$ and $B(E2)$ values, respectively, allows one to assign the deformation parameter $\beta = 0.14$ to the ground-state band of ^{140}Xe. The moments obtained within the collective model are somewhat constant for the lower part of the ground-state band, corresponding to transition rates of the order of 20–30 W.u. The intrinsic quadrupole moment of the ground state calculated from $E2$ matrix elements yields 232 e fm^2, which agrees well with values presented in Table V and approaches closely the pseudo-SU3 estimate of 233 e fm^2.

A characteristic feature of a γ band is a low-lying 3^+ level. This was predicted [1] and observed [4] in the vicinity of the

^{78}Ni core and is now evidenced in the ^{132}Sn region because of the unique assignment of the 3^+ spin and parity to the 1304.6-keV level in ^{140}Xe. Indeed, in both ^{138}Te and ^{140}Xe, the shell model predicts development of γ bands. Strong $B(E2; 3^+ \rightarrow 2_2^+)$ transition rates as well as the quadrupole moments of the 2_1^+ and 2_2^+ levels of nearly equal values and opposite signs indicate triaxiality in both nuclei. Especially in ^{140}Xe the enhanced collectivity leads to a distinct γ band, seen in Fig. 11 as a sequence of states, connected by strong transitions, with $B(E2; 3^+ \rightarrow 2_2^+)$ of 44 W.u. The (β,γ) deformation parameters estimated from the calculated $E2$ matrix elements within the aforementioned method from Ref. [23] are $(0.11, 9^\circ)$ and $(0.15, 15.5^\circ)$ for the ground state of ^{138}Te and ^{140}Xe, respectively, supporting stronger collectivity and nonaxiality in ^{140}Xe as compared to ^{138}Te.

We note that the 1323.4-keV (2^+) level in ^{138}Te, reported in Ref. [14] is well reproduced in our calculations and there are also experimental candidates in Ref. [14] for the 3^+ level, calculated at 1521 keV.

IV. CONCLUSIONS

In summary, we have observed for the first time excitations corresponding to γ collectivity close to the ^{132}Sn core. New excited levels found in the $N = 86$ isotones ^{138}Te and ^{140}Xe can be interpreted as members of γ bands. A γ band is clearly present in ^{140}Xe where we uniquely assigned spin and parity of $I^\pi = 3^+$, $I^\pi = 5^+$, and $I^\pi = 7^+$ to the 1304.6-, 1573.1-, and 1954.6-keV levels, respectively. In ^{138}Te, the $I^\pi = 7^+$ assignment to the 2021.8-keV level allows one to propose an analogous γ band because of similarities between excitation schemes of ^{138}Te and ^{140}Xe. The collectivity observed in the ground-state band and in the proposed γ band of the ^{138}Te nucleus, having only two valence protons and four valence neutrons, is the closest such effect to the ^{132}Sn doubly magic core.

The proposed interpretation is supported by large-scale, shell-model calculations performed in this work for ^{138}Te and ^{140}Xe. The calculations reproduce well the structure of excitations in the two nuclei and the collectivity in both the ground-state cascades and the new γ bands. The evolution of the collectivity in the ^{132}Sn region is sensitive to the single-particle splitting, especially between the $d_{5/2}$ and $g_{7/2}$ proton orbital. Therefore, the present study can serve as a benchmark for the shell-model parametrization in this region.

It is of interest to verify further the degree of collectivity close to the ^{132}Sn core as well as the possible coexistence and mixing of collective and single-particle structures in these nuclei. The 4^+, 5^+, and 6^+ spin and parity assignments to the respective 1617.4-, 1774.2-, and 1863.2-keV levels in ^{138}Te should be confirmed. One should also explain the trend of the excitation energies in γ bands of the $N = 86$ isotones, seen in Fig. 9(b). It is changing at ^{140}Xe, which may indicate mixing around spin 8^+ between single-particle and collective structures, especially in ^{138}Te. Finally, it is important to uniquely identify low-spin members of γ bands in ^{138}Te, ^{140}Xe and to search for γ bands in heavier $N = 86$ isotones.

ACKNOWLEDGMENTS

This material is based upon work supported by the US Department of Energy, Office of Science, Office of Nuclear Physics, under Contract No. DE-AC02-06CH11357. The authors are grateful for the use of ^{248}Cm to the Office of Basic Energy Sciences, US Department of Energy, through the transplutonium element production facilities at Oak Ridge National Laboratory. H.N. acknowledges support from the Helmholtz association through the Nuclear Astrophysics Virtual Institute NAVI (Grant No. VH-VI-417).

[1] K. Sieja, T. R. Rodriguez, K. Kolos, and D. Verney, Phys. Rev. C **88**, 034327 (2013).

[2] T. Rząca-Urban, M. Czerwiński, W. Urban, A. G. Smith, I. Ahmad, F. Nowacki, and K. Sieja, Phys. Rev. C **88**, 034302 (2013).

[3] K. Kolos, D. Verney, F. Ibrahim, F. Le Blanc, S. Franchoo, K. Sieja, F. Nowacki, C. Bonin, M. Cheikh Mhamed, P. V. Cuong, F. Didierjean, G. Duchêne, S. Essabaa, G. Germogli, L. H. Khiem, C. Lau, I. Matea, M. Niikura, B. Roussi'ere, I. Stefan, D. Testov, and J.-C. Thomas, Phys. Rev. C **88**, 047301 (2013).

[4] T. Materna, W. Urban, K. Sieja, U. Köster, H. Faust, M. Czerwiński, T. Rząca-Urban, C. Bernards, C. Fransen, J. Jolie, J.-M. Regis, T. Thomas, and N. Warr, Phys. Rev. C **92**, 034305 (2015).

[5] J.-P. Delaroche, M. Girod, J. Libert, H. Goutte, S. Hilaire, S. Péru, N. Pillet, and G. F. Bertsch, Phys. Rev. C **81**, 014303 (2010).

[6] P. J. Nolan, F. A. Beck, and D. B. Fossan, Annu. Rev. Nucl. Part. Sci. **44**, 561 (1994).

[7] W. Urban, J. L. Durell, W. R. Phillips, A. G. Smith, M. A. Jones, I. Ahmad, A. R. Barnett, M. Bentaleb, S. J. Dorning, M. J. Leddy, E. Lubkiewicz, L. R. Morss, T. Rząca-Urban, R. A. Sareen, N. Shulz, and B. J. Varley, Z. Phys. A **358**, 145 (1997).

[8] T. Rząca-Urban, W. Urban, A. G. Smith, I. Ahmad, and A. Syntfeld-Każuch, Phys. Rev. C **87**, 031305(R) (2013).

[9] F. Hoellinger, B. J. P. Gall,N. Schulz, W. Urban, I. Ahmad, M. Bentaleb, J. L. Durell, M. A. Jones, M. J. Leddy, E. Lubkiewicz, L. R. Morss, W. R. Phillips, A. G. Smith, and B. J. Varley, Eur. Phys. J. A **6**, 375 (1999).

[10] M. Bentaleb, N. Schulz, E. Lubkiewicz, J. L. Durell, C. J. Pearson, W. R. Phillips, J. Shannon, B. J. Varley, I. Ahmad, C. J. Lister, L. R. Morss, K. L. Nash, and C. W. Williams, Z. Phys. A **354**, 143 (1996).

[11] J. H. Hamilton, A. V. Ramayya, J. K. Hwang, J. Kormicki, B. R. S. Babu, A. Sandulescu, A. Florescu, W. Greiner, G. M. Ter-Akopian, Yu. Ts. 0ganessian, A. V. Daniel, S. J. Zhu *et al.*, Prog. Part. Nucl. Phys. **38**, 273 (1997).

[12] W. Urban, T. Rząca-Urban, N. Shulz, J. L. Durell, W. R. Phillips, A. G. Smith, B. J. Varley, and I. Ahmad, Eur. Phys. J. A **16**, 303 (2003).

[13] W. Urban, W. R. Phillips, N. Schulz, B. J. P. Gall, I. Ahmad, M. Bentaleb, J. L. Durell, M. A. Jones, M. J. Leddy, E. Lubkiewicz, L. R. Morss, A. G. Smith, and B. J. Varley, Phys. Rev. C **62**, 044315 (2000).

[14] P. Lee, C.-B. Moon, C. S. Lee, A. Odahara, R. Lozeva, A. Yagi, S. Nishimura, P. Doornenbal, G. Lorusso, P.-A. Söderström *et al.*, Phys. Rev. C **92**, 044320 (2015).
[15] C. Xing-Lai, Z. Sheng-Jiang, J. H. Hamilton, A. V. Ramayya, J. K. Hwang, U. Yong-Nam, L. I. Ming-Liang, Zheng Rang-Chen, I. Y. Lee, J. O. Rasmussen, Y. X. Luo, and W. C. Ma, Chin. Phys. Lett. **21**, 1904 (2004).
[16] I. Ahmad and W. R. Phillips, Rep. Prog. Phys. **58**, 1415 (1995).
[17] W. Urban, R. M. Lieder, J. C. Bacelar, P. P. Singh, D. Alber, D. Balabanski, W. Gast, H. Grawe, G. Hebbibnghaus, J. R. Jongman *et al.*, Phys. Lett. B **258**, 293 (1991).
[18] W. Urban, M. A. Jones, J. L. Durell, M. Leddy, W. R. Phillips, A. G. Smith, B. J. Varley, I. Ahmad, L. R. Morss, M. Bentaleb, E. Lubkiewicz, and N. Shulz, Nucl. Phys. A **613**, 107 (1997).
[19] E. Caurier and F. Nowacki, Acta Phys. Pol. B **30**, 705 (1999).
[20] E. Caurier, G. Martinez-Pinedo, F. Nowacki, A. Poves, and A. Zuker, Rev. Mod. Phys. **77**, 427 (2005).
[21] K. Sieja, Acta Phys. Pol. B **47**, 1001 (2016).
[22] A. Lindroth, B. Fogelberg, H. Mach, M. Sanchez-Vega, and J. Bielcik, Phys. Rev. Lett. **82**, 4783 (1999).
[23] K. Kumar, Phys. Rev. Lett. **28**, 249 (1972).